EPJ Web of Conferences **239**, 03004 (2020) https://doi.org/10.1051/epjconf/202023903004
ND2019

Validating the Bohr hypothesis: Comparing fission-product yields from photon-induced fission of ^{240}Pu and neutron-induced fission of ^{239}Pu

Jack Silano[1,*], *Anton* Tonchev[1,2], *Roger* Henderson[1], *Nicolas* Schunck[1], *Werner* Tornow[2,3], *Calvin* Howell[2,3], *FNU* Krishichayan[2,3], and *Sean* Finch[2,3]

[1]Nuclear and Chemical Sciences Division, Lawrence Livermore National Laboratory, Livermore, CA 94550, USA
[2]Duke University, Department of Physics, Box 90308, Durham, NC 27708-0308, USA
[3]Triangle Universities Nuclear Laboratory, Durham, NC 27708, USA

Abstract. The Bohr hypothesis, one of the most fundamental assumptions in nuclear fission theory, states that the decay of a compound nucleus with a given excitation energy, spin and parity is independent of its formation. Using fission product yields (FPYs) as a sensitive probe, we have performed new high precision test of the combined effects of the entrance channel, spin and parity on the fission process. Two different reactions were used in a self-consistent manner to produce a compound ^{240}Pu nucleus with the same excitation energy: neutron induced fission of ^{239}Pu at $E_n = 4.6$ MeV and photon-induced fission of ^{240}Pu at $E_\gamma = 11.2$ MeV. The FPYs from these two reactions were measured using quasimonoenergetic neutron beams from the TUNL's FN tandem Van de Graaff accelerator and quasimonenergetic photon beams from the High Intensity γ-ray Source (HIγS) facility. The first results comparing the FPYs from these two reactions will be presented. Implications for validating the Bohr hypothesis will be discussed.

1 Introduction

In 1939, Niels Bohr and John Wheeler formulated a theory of neutron-induced nuclear fission based on the hypothesis of the compound nucleus [1]. The "Bohr hypothesis" is at the heart of every current theoretical fission model; it states that the decay of a compound nucleus for a given excitation energy, spin, and parity is independent of its formation [2]. The timescale for the formation of the compound nucleus ($\sim 10^{-16}$ seconds) is long enough for a nucleon to traverse the nucleus $\sim 10^7$ times. Thus there is sufficient time for the compound nucleus to "forget" the details of its origin. Although this hypothesis is widely accepted by theorists and experimentalists, its implications (especially concerning fission product yields) have never been experimentally verified precisely via direct comparison of fission observables. Currently, the Bohr hypothesis is verified to about 20% accuracy in nuclear reactions such as (t,pf), (^{3}He,df), and (^{3}He,tf) [3–7]. We performed direct experimental validation of the practical consequences of the Bohr hypothesis during induced nuclear fission. We compared the fission product yields (FPYs) of the same ^{240}Pu compound nucleus produced by two different reactions: (i) n+^{239}Pu and (ii) γ+^{240}Pu. The two Pu isotopes provided a valuable set of nuclides for use in investigating the influence of the spin and parity of the compound nucleus on the detailed fission product yields distribution, including shell and pairing effects and fission dynamics. The only difference between these two reactions was a small mismatch in the spin and parity distributions of the ^{240}Pu compound nucleus. High-precision measurements of the ^{240}Pu fission product yields using monoenergetic photons produced at the High Intensity γ-ray Source (HIγS) facility were performed using a γ-ray beam energy of 11.2 MeV, creating the same compound nucleus and excitation energy as neutron-induced fission of ^{239}Pu at an incident neutron energy of 4.6 MeV.

*e-mail: silano1@llnl.gov

1.1 Fission product-yield relevance

Nuclear fission, the most pronounced collective nuclear-structure phenomenon, relates the fission product yields and their kinetic energies to the potential energy of the fission system [8]. The evolution of the fission system (from the initial particle impact through intermediate saddle points to scission and finally to the configuration of separated fission fragments) is governed by multidimensional potential-energy surfaces and the shell structure of the fragments. At low excitation energies, shell and pairing effects in nuclei influence both the mass and energy distribution of the fission fragments; therefore, nuclear structure details are required to describe experimental fission data. Models based on different phenomenological and microscopic approaches are used to describe the complexity of the fission process and are assessed by how well they describe the various experimental observables [9]. One of these observables is the dependence of the FPYs on the excitation energy of the compound nucleus. The magnitude and the slope of the energy dependencies of the FPYs have significant impacts on basic and applied physics. For example, r-process nucleosynthesis cannot be fully understood without a precise knowledge of the fission properties of very neutron-rich isotopes of the heaviest elements, which are presently not accessible to direct measurements [10]. Precise knowledge of FPYs is critical to nuclear reactor operation, nondestructive nuclear fuel investigation, accelerator-driven systems, and decay heat [11–14]. In addition, information about the FPYs has a fundamental impact on basic fission studies and the antineutrino spectrum [15]. The accuracy of purely theoretical predictions is insufficient for quantitative predictions of the energy dependence of FPYs on the precision that present nuclear applications require [16]. However, it is very difficult to make quantitative predictions about the FPYs, especially within a microscopic approach based on time-dependent Hartree-Fock calculations, where the experimental magnitude of the energy dependence is comparable to (or even smaller than) the uncertainties of the theoretically calculated FPYs [17, 18].

2 Experiment

We performed the first-ever experiment to identify the practical consequences of the Bohr hypothesis in the context of induced nuclear fission. We measured the FPYs from the ^{240}Pu(γ,f) reaction at the HIγS facility at Triangle Universities Nuclear Laboratory (TUNL) [19] and compared the results to the FPYs obtained from the ^{239}Pu(n,f) reaction that our group recently measured at the TUNL Tandem Van de Graaff accelerator [20–23]. As shown in Fig. 1, both reactions produced a ^{240}Pu compound nucleus with the same excitation energy since the energies of the incident neutron and photon beams were carefully chosen to account for the 6.5 MeV difference in binding energy between ^{239}Pu and ^{240}Pu. The only difference was the spin-parity distributions from n + ^{239}Pu and $J^\pi = 1^-$ from γ + ^{240}Pu, which is widely believed to be inconsequential at high excitation energies.

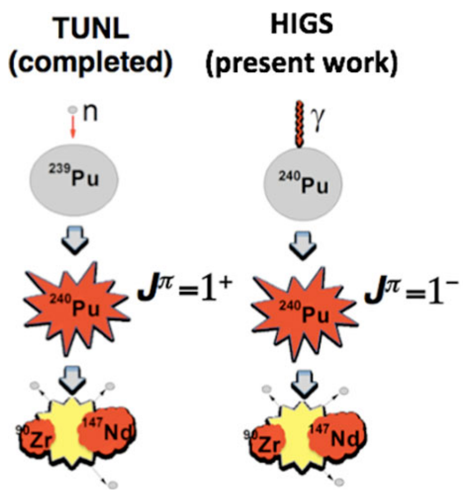

Figure 1. A schematic representation of the experimental technique. An excited, compound ^{240}Pu nucleus will be created through two different nuclear reactions: n + ^{239}Pu and γ + ^{240}Pu. The compound nucleus will then decay via fission, and the FPYs will be used to probe the similarity of the two reactions.

2.1 Dual-fission chambers

One of the most significant components in measurements of fission product yields is determining the number of fission reactions that occurred in the target. In the present work the fission reactions are counted using a Dual-fission ionization Chamber (DFC) [20], based on the design by Grundl *et al.* [24] for FPY measurements in reactors and critical assemblies [25].

The irradiation for the ^{239}Pu(n,f) measurements in Gooden *et al.* [22] were performed with the thick ^{239}Pu activation target mounted in the center of the DFC, as is the standard procedure used by our group [20–22, 26]. The two FCs then measure the effective neutron flux just before and after the target, and the effects of the beam divergence can be accounted for with Monte Carlo calculations [20]. The previously published data for ^{239}Pu(n,f) at E_n = 4.6 MeV were augmented with a new recent measurement using the same experimental procedure and target but with only 2 hours of irradiation, in order to measure the yields of FPYs with half lives of a few minutes to a few hours.

In the case of the ^{240}Pu photofission measurements, the thick ^{240}Pu activation targets were positioned just outside of the DFC, with the long-activation target upstream and the short-activation target downstream with respect to the γ-ray beam. Unlike the neutron beams at TUNL, the HIγS γ-ray beam is highly parallel with negligible divergence over a few cm distance. Thus it is not necessary to account for the spread of the γ-ray beam between the FC and the targets. This assumption was confirmed by comparing the relative beam flux measured in each chamber in the DFC. When a DFC is mounted in the neutron beam at TUNL, the beam divergence causes the upstream FC to typically see ~ 25% greater flux than the downstream FC, after accounting for the masses of the reference foils in each chamber. In the HIγS γ-ray beam, the ^{240}Pu DFC upstream to downstream FC ratio of 1.02 ± 0.01 was reasonably consistent with negligible γ-ray beam divergence.

2.2 Activation targets & reference foils

The ^{240}Pu targets used in this measurement (see Table 1) both consist of ^{240}PuO$_2$ powder which is compressed into a 1.27 cm diameter Al cylinder, the same diameter as the ^{239}Pu target that was used in Ref. [22]. The Al holders have a mass of ~ 19 mg, with a 1.91 cm outer diameter and a 0.191 cm thickness. The Al material is relatively transparent to the γ-rays emitted by the β-decay of fission products and also is not activated by exposure to the 11.2 MeV γ-ray beam.

The reference foils for the DFC (see Table 2) consist of ^{240}Pu electroplated onto a 1.27 cm diameter area on a Ti backing. Like the ^{239}Pu reference foils, the ^{240}Pu deposits were sufficiently thin that fission fragments could easily escape the foil and deposit their energy in the gas of the ionization chambers with nearly 100% efficiency.

Target	Mass (mg)	Isotopic Enrichment (%)
^{240}Pu #1	73.01±0.04	99.873
^{240}Pu #2	89.11±0.05	99.873

Table 1. ^{240}Pu activation target targets used in this work.

Target	Mass (μg)	Isotopic Enrichment (%)
^{240}Pu #3	25.97±0.18	99.873
^{240}Pu #4	23.60±0.12	99.873

Table 2. ^{240}Pu electroplated reference foils used in the DFCs in this work.

2.3 Monoenergetic photon beams from the HIγS facility

The HIγS facility produces intense, quasimonoenergetic γ-ray beams via intra-cavity Compton backscattering of free electron laser photons and relativistic electrons [19]. Photofission measurements require intense γ-ray beams such as the ones provided by the HIγS facility since the (γ,f) reaction is typically a factor of ~5–10 less than the (n,f) reaction for a given target nucleus.

For this work, the HIγS facility was operated using 540 nm free electron laser photons to produce linearly-polarized, 11.2 MeV γ-ray beams with a resolution of approximately 360 keV (FWHM) and an average flux on target of 1.95×10^7 γ-rays/(cm^2 s). The γ-ray beam was collimated with a 1.27 cm diameter, 15.24 cm long Pb collimator placed ~2.5 m upstream of the target assembly. The energy spectrum of the γ-ray beam was measured with a 123% high-purity germanium (HPGe) detector positioned in the beam axis, while copper attenuators were inserted into the γ-ray beam far upstream of the collimator to reduce the flux.

One ^{240}Pu target (#1) was irradiated with E_γ=11.2 MeV γ-ray beam for 2 hours to measure the short-lived FPYs, the other (#2) for 92.6 hours to build up activity of long-lived FPYs. The 2 hour irradiation induced a total of $8.25 \pm 0.15 \times 10^6$ fissions in the short-lived FPY target, while the 92.6 hour irradiation induced a total of $4.38 \pm 0.07 \times 10^8$ fission events.

2.4 Detection of γ-rays from the β-decay of fission products

After irradiation by the HIγS γ-ray beam, the activated ^{240}Pu targets were monitored by a 60% relative efficiency HPGe. The first target with 2 hours of irradiation was counted for ~ 90 hours while the second, long-lived FPY target was being irradiated. After the long irradiation was completed, the second ^{240}Pu target replaced the first one in the HPGe counting station. Thus both ^{240}Pu targets were monitored by the same HPGe at the same distance. Since this HPGe is the same one that was used in the ^{239}Pu(n,f) measurements in Gooden *et al.* [22] (and in the supplemental ^{239}Pu(n,f) measurements made recently), all of the FPY measurements are on the same systematic footing. Consequently this work posseses a unique sensitivity for comparing FPY distributions from the ^{239}Pu(n,f) and ^{240}Pu(γ,f) reactions. The measured fission product γ-ray spectra from the ^{239}Pu(n,f) and ^{240}Pu(γ,f) reactions are compared in Fig. 2.

2.5 Analysis & data reduction

Yields of specific fission products are determined by counting γ-rays emitted by their decay. Choosing the counting window in time is complicated by the interplay of the activity of the γ-ray of interest, interfering background peaks and the smooth continuum background. Because all of these features are time dependent, it can be difficult to predict a priori what the ideal integral time window is to fit the net photopeak area. In this work, a procedure was developed to automatically determine the integration time in a way which minimizes the uncertainty in the net photopeak counts, which is often one of the largest sources of uncertainty in the short-lived FPY measurements. Multiple spectra were generated with each successive spectrum having a longer counting time. The photopeak of interest was fit in each spectrum with a Gaussian function, including a linear background and other Gaussian peaks. The uncertainty of the net photopeak counts from the fit was then plotted as a function of counting time. In addition to minimizing the uncertainty in the photopeak counts, this method removes the choice of the counting period as a potential source of bias. As shown in Fig. 3, the uncertainty initially decreases with counting time as the photopeak statistics increase, but then begins to increase as the background builds up faster than the diminishing peak activity. In this example, the peak counts uncertainty is minimized with a counting time of ~ 1.5 hours.

Using the same formalism as in Ref. [22], the FPYs can be defined as:

$$\mathrm{FPY}_i = \frac{\lambda_i N_i}{F_T N_a I_{\gamma i} \epsilon_i} \frac{1}{1 - e^{-\lambda_i t_e}} \frac{1}{e^{-\lambda_i t_d}} \cdot \frac{1}{1 - e^{-\lambda_i t_m}} \prod_k C_{ki}, \quad (1)$$

where

$$\begin{aligned}
\lambda_i &= \text{Decay constant} \\
N_i &= \text{Number of } \gamma\text{-rays from photopeak} \\
N_a &= \text{Number of target nuclei} \\
I_{\gamma i} &= \text{Branching ratio} \\
\epsilon_i &= \text{Full energy peak efficiency of HPGe detector} \\
F_T &= \text{Fission rate in target determined from the DFC} \\
t_e &= \text{Time of beam exposure} \\
t_d &= \text{Decay time from end of activation} \\
t_m &= \text{Target measurement time} \\
C_{ki} &= \text{Correction factors}
\end{aligned} \quad (2)$$

The correction factors include effects due to beam fluctuations, γ-ray attenuation and summing in the HPGe.

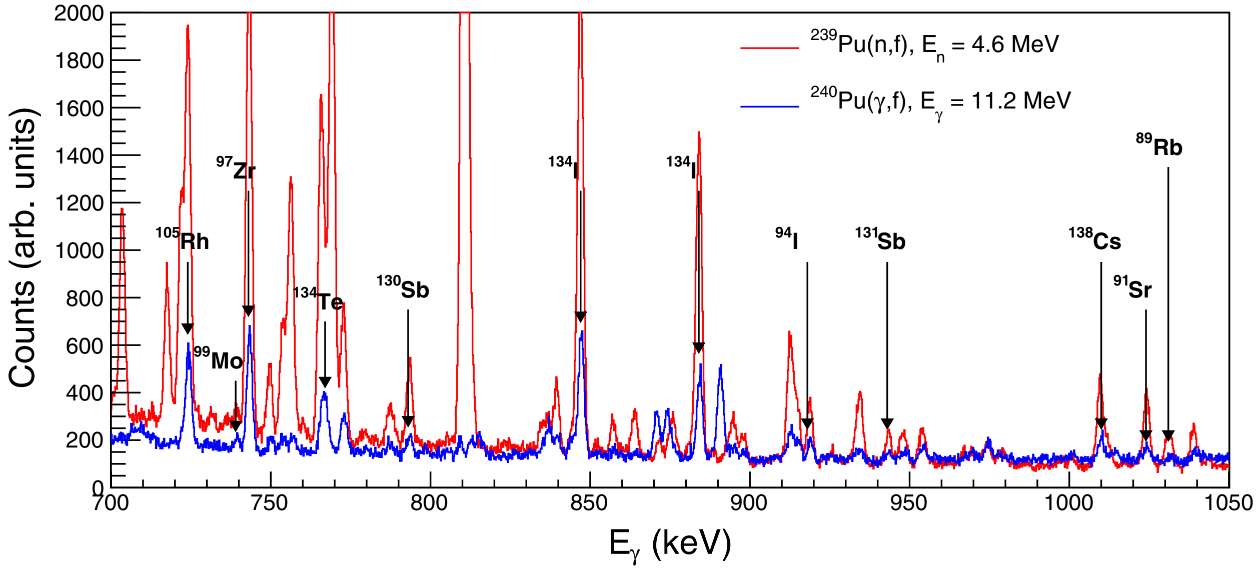

Figure 2. γ-ray spectra from fission products from ^{240}Pu(γ,f) at E_γ = 11.2 MeV and ^{239}Pu(n,f) at E_n = 4.6 MeV, measured by a 60% relative efficiency HPGe. Both spectra come from targets which were irradiated for 2 hours.

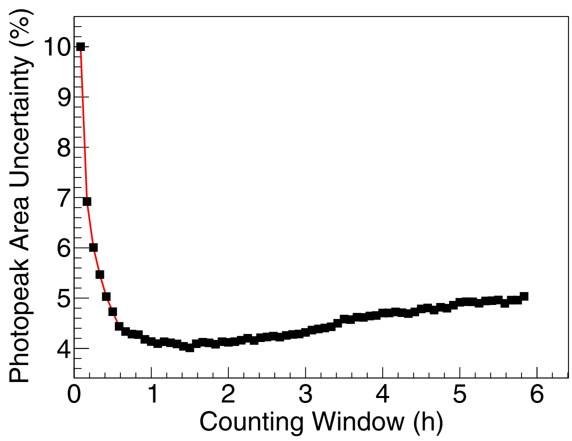

Figure 3. The uncertainty in the net photopeak counts as a function of counting time for the 302.77 keV γ-ray emitted by the decay of ^{107}Rh in the ^{240}Pu(γ,f) FPY spectrum.

3 Results & discussion

The 30 unique FPYs measured from ^{240}Pu(γ,f) at E_γ = 11.2 MeV are plotted in Fig. 4 along with the corresponding yields from ^{239}Pu(n,f) at E_n = 4.6 MeV, if available. There were 22 unique FPYs which were measured for both sets of data. The FPYs are generally in good agreement, though there are some notable differences where the yields differ by multiple standard deviations. Significantly, the light mass peak in the FPY distribution doesn't show a systematic shift between the two distributions. Such a shift is expected in the case where the fissioning compound nucleus has a different mass, as the heavy fragment tends to remain constant due to shell closures, and additional nucleons are added to the light fragment. The lack of a systematic difference between the two FPY distributions is consistent with Bohr's hypothesis.

We plan to compare the FPYs from ^{240}Pu(γ,f) at E_γ = 11.2 MeV with those from ^{239}Pu(n,f) at different incident neutron energies to determine the impact of the angular momentum and excitation energy of the entrance channel. The similarity of the FPYs from both reactions at the same excitation energy indicates the validity of the Weisskopf-Ewing limit [27] in which the fission probability is independent of the spin and parity of the compound nuclear system. This limit holds when the excitation energy is high enough for the decay widths to be dominated by the statistical level density, which is the case in the present work. A planned measurement of the FPYs from ^{240}Pu(γ,f) at E_γ = 8 MeV, to be compared with existing FPY data from ^{239}Pu(n,f) at E_n = 1.4 MeV [22], will probe the similarity of the yields at an excitation energy for which the Weisskopf-Ewing limit is not valid due to the lower density of states.

4 Conclusion

This work represents the first comparison of FPYs from ^{240}Pu(γ,f) to the FPYs of ^{239}Pu(n,f). Since both measurements were performed with the same experimental techniques and exact same HPGe, these data sets are unaffected by many sources of systematic error and are thus a uniquely sensitive probe of the role of the entrance channel on the fission process. Future photofission measurements at additional E_γ could investigate if the similarity between the yields evolves with excitation energy, further testing Bohr's hypothesis in the context of nuclear fission.

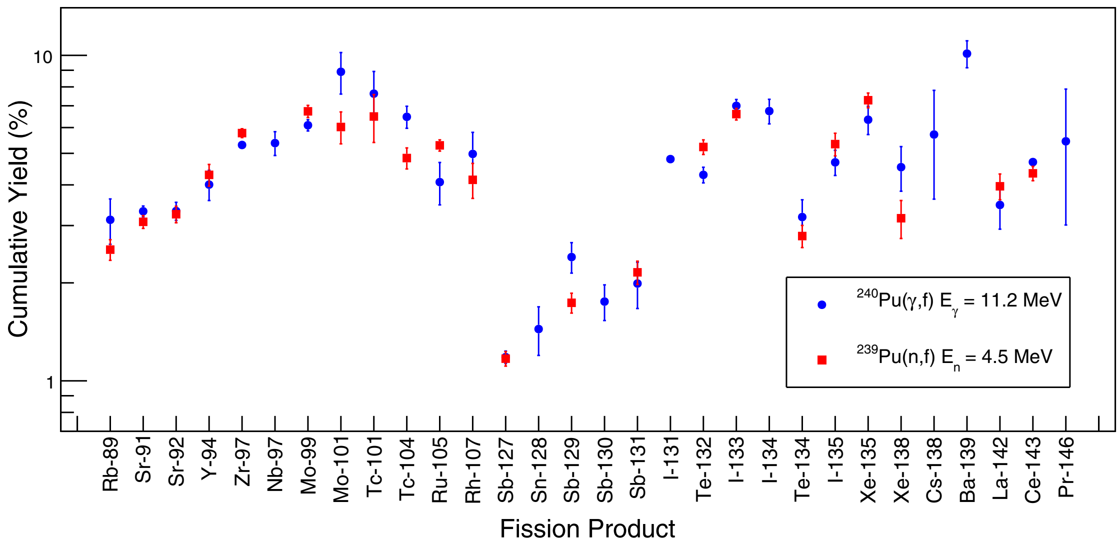

Figure 4. Preliminary FPYs from ^{240}Pu(γ,f) at E_γ = 11.2 MeV and ^{239}Pu(n,f) at E_n = 4.6 MeV. The ^{239}Pu(n,f) FPYs include new measurements of short-lived FPYs in combination with long-lived FPYs from Gooden *et al.* [22]

Acknowledgements

We would like to thank the HIγS staff for delivering excellent quality γ-ray beams for this work. This work was performed under the auspices of the U.S. Department of Energy by Lawrence Livermore National Laboratory under Contract DE-AC52-07NA27344. This work was also supported partially by the U.S. Department of Energy, Office of Nuclear Physics, under Grant No. DE-FG02-97ER41033, and by the National Nuclear Security Administration under the Stewardship Science Academic Alliance Program through the U.S. Department of Energy, Grants No. DE-NA0002793, DE-NA0002936, DE-NA0003884 and DE-NA0003887.

References

[1] N. Bohr, Phys. Rev. **56**, 426 (1939)
[2] N. Bohr, Nature **137**, 344 (1936)
[3] H.C. Britt, F.A. Rickey, W.S. Hall, Phys. Rev. **175**, 1525 (1968)
[4] J.D. Cramer, H.C. Britt, Phys. Rev. C **2**, 2350 (1970)
[5] H.C. Britt, J.D. Cramer, Phys. Rev. C **2**, 1758 (1970)
[6] W. Younes, H.C. Britt, Phys. Rev. C **67**, 024610 (2003)
[7] W. Younes, Phys. Rev. C **68** (2003)
[8] R. Vandenbosch, J. Huizenga, Press, New York (1973)
[9] C. Wagemans, *The nuclear fission process* (CRC press, 1991)
[10] C. Iliadis, *Nuclear physics of stars* (John Wiley & Sons, 2015)
[11] M. Chadwick, T. Kawano, D. Barr, M.M. Innes, A. Kahler, T. Graves, H. Selby, C. Burns, W. Inkret, A. Keksis et al., Nucl. Data Sheets **111**, 2923 (2010)
[12] J. Laurec, A. Adam, T. de Bruyne, E. Bauge, T. Granier, J. Aupiais, O. Bersillon, G.L. Petit, N. Authier, P. Casoli, Nucl. Data Sheets **111**, 2965 (2010)
[13] M.M. Innes, M. Chadwick, T. Kawano, Nucl. Data Sheets **112**, 3135 (2011)
[14] D.R. Nethaway, A.L. Prindle, W.A. Myers, W.C. Fuqua, M.V. Kantelo, Phys. Rev. C **16**, 1907 (1977)
[15] A.C. Hayes, J.L. Friar, G.T. Garvey, G. Jungman, G. Jonkmans, Phys. Rev. Lett. **112**, 202501 (2014)
[16] K.H. Schmidt, A. Kelić, M.V. Ricciardi, Europhys. Lett. **83**, 32001 (2008)
[17] N. Schunck, D. Duke, H. Carr, Phys. Rev. C **91**, 034327 (2015)
[18] J. Randrup, P. Möller, Phys. Rev. C **88**, 064606 (2013)
[19] H.R. Weller, M.W. Ahmed, H. Gao, W. Tornow, Y.K. Wu, M. Gai, R. Miskimen, Prog. Part. Nucl. Phys. **62**, 257 (2009)
[20] C. Bhatia, B. Fallin, M. Gooden, C. Howell, J. Kelley, W. Tornow, C. Arnold, E. Bond, T. Bredeweg, M. Fowler et al., Nucl. Instrum. Methods Phys. Res., Sect. A **757**, 7 (2014)
[21] C. Bhatia, B.F. Fallin, M.E. Gooden, C.R. Howell, J.H. Kelley, W. Tornow, C.W. Arnold, E. Bond, T.A. Bredeweg, M.M. Fowler et al., Phys. Rev. C **91**, 064604 (2015)
[22] M. Gooden, C. Arnold, J. Becker, C. Bhatia, M. Bhike, E. Bond, T. Bredeweg, B. Fallin, M. Fowler, C. Howell et al., Nucl. Data Sheets **131**, 319 (2016)
[23] A. Tonchev, M. Stoyer, J. Becker, R. Macri, C. Ryan, S. Sheets, M. Gooden, C. Arnold, E. Bond, T. Bredeweg et al., *Energy Evolution of the Fission-Product Yields from Neutron-Induced Fission of 235U, 238U, and 239Pu: An Unexpected Observation*, in *Fission and Properties of Neutron-Rich Nuclei* (WORLD SCIENTIFIC, 2017), ISBN 9789813229426

[24] J.A. Grundl, D.M. Gilliam, N.D. Dudey, R.J. Popek, Nucl. Technol. **25**, 237 (1975)
[25] H. Selby, M.M. Innes, D. Barr, A. Keksis, R. Meade, C. Burns, M. Chadwick, T. Wallstrom, Nucl. Data Sheets **111**, 2891 (2010)
[26] C. Bhatia, B. Fallin, C. Howell, W. Tornow, M. Gooden, J. Kelley, C. Arnold, E. Bond, T. Bredeweg, M. Fowler et al., Nucl. Data Sheets **119**, 324 (2014)
[27] V.F. Weisskopf, Phys. Rev. **57**, 472 (1940)